Structure of the Extended-Spectrum Class C β-Lactamase of *Enterobacter cloacae* GC1, a Natural Mutant with a Tandem Tripeptide Insertion[†,‡]

Gregg V. Crichlow,[§] Alexandre P. Kuzin,[§] Michiyoshi Nukaga,[||] Kayoko Mayama,[||] Tetsuo Sawai,[||] and James R. Knox*[,§]

Department of Molecular and Cell Biology, The University of Connecticut, Storrs, Connecticut 06269-3125, and Faculty of Pharmaceutical Sciences, Chiba University, Chiba 263, Japan

Received April 15, 1999; Revised Manuscript Received June 7, 1999

ABSTRACT: A class C β-lactamase from a clinical isolate of *Enterobacter cloacae* strain GC1 with improved hydrolytic activity for oxyimino β-lactam antibiotics has been analyzed by X-ray crystallography to 1.8 Å resolution. Relative to the wild-type P99 β-lactamase, this natural mutant contains a highly unique tandem repeat Ala211-Val212-Arg213 [Nugaka et al. (1995) *J. Biol. Chem. 270*, 5729−5735]. The 39.4 kDa chromosomal β-lactamase crystallizes from poly(ethylene glycol) 8000 in potassium phosphate in space group $P2_12_12$ with cell dimensions $a = 78.0$ Å, $b = 69.5$ Å, and $c = 63.1$ Å. The crystal structure was solved by the molecular replacement method, and the model has been refined to an *R*-factor of 0.20 for all nonzero data from 8 to 1.8 Å. Deviations of model bonds and angles from ideal values are 0.008 Å and 1.4°, respectively. Overlay of α-carbon atoms in the GC1 and P99 β-lactamases results in an rms deviation of 0.6 Å. Largest deviations occur in a loop containing Gln120 and in the Ω loop region (200−218) where the three residues 213−215 are disordered. Possibly as a result of this disorder, the width of the opening to the substrate binding cavity, as measured from the 318−324 β-strand to two loops containing Gln120 and Tyr150 on the other side, is 0.6−1.4 Å wider than in P99. It is suggested that conformational flexibility in the expanded Ω loop, and its influence on adjacent protein structure, may facilitate hydrolysis of oxyimino β-lactams by making the acyl intermediate more open to attack by water. Nevertheless, backbone atoms in core catalytic site residues Ser64, Lys67, Tyr150, Asn152, Lys318, and Ser321 deviate only 0.4 Å (rmsd) from atoms in P99. A rotation of a potential catalytic base, Tyr150, relative to P99 at pH 8, is consistent with the requirement for a lower than normal pK_a for this residue.

Serine-reactive β-lactamases (EC 3.5.2.6, classes A, C, and D) function via an acyl intermediate to hydrolyze the β-lactam bond in β-lactam antibiotics (*1, 2*). These enzymes, as well as a smaller group of zinc-reactive β-lactamases (class B), are the principal agents of bacterial resistance to many penicillins, cephalosporins, and monobactams (*3*−*5*).

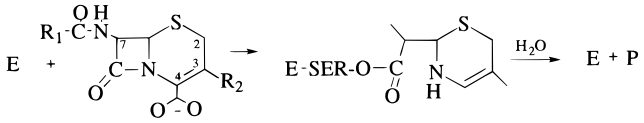

Many wild-type class C enzymes (or cephalosporinases) are made especially effective by a high level of β-lactam-inducible overproduction, but constitutive production is common in clinical isolates highly resistant to β-lactams. *Enterobacter cloacae* strain GC1, a Gram-negative pathogen isolated from a patient in 1992 in Japan, was found to produce a constitutive class C β-lactamase with extended substrate specificity for oxyimino cephalosporins and monobactams (*6*). Though extended specificity is now well-known for plasmid-derived class A β-lactamases (*7, 8*), this report was the first example of a chromosomal class C extended-spectrum β-lactamase. The k_{cat} values of the GC1 β-lactamase for aztreonam, ceftazidime, and cefuroxime were increased 100−1000-fold compared with the wild-type *E. cloacae* P99 β-lactamase, the species-specific class C enzyme that lacks an extended specificity. The 364-residue GC1 β-lactamase differs from the P99 β-lactamase by five amino acids, but the extended specificity of the GC1 enzyme was thought to be entirely due to only three residues in a tripeptide insertion, a highly unusual tandem duplication of Ala208-Val209-Arg210. From mutagenesis experiments, it was concluded that the length of the insertion, rather than the sequence, is somehow pivotal in the function of this mutant β-lactamase (*6, 9*). The kinetic characteristics of the GC1 β-lactamase and its engineered mutants suggested that the cause of the more effective hydrolysis of newer cephalosporins and monobactams is a decreased stability of acyl-enzyme oxyimino intermediates.

On the basis of the known crystallographic structure of the wild-type P99 β-lactamase at 2 Å resolution (*10*), the tripeptide insertion in GC1 would occur in the middle of a so-called Ω loop (189−226) that forms a wall of the cephalosporin binding cavity. Here we report the crystal

[†] This work was supported by grants from the Suntory Institute for Bioorganic Research and the Naito Foundation (to M.N.).

[‡] Atomic coordinates have been deposited in the Protein Data Bank (entry 1GCE) at Rutgers University.

* Corresponding author: phone 860-486-3133; fax 860-486-4745; e-mail knox@uconnvm.uconn.edu.

[§] The University of Connecticut.

[||] Chiba University.

10.1021/bi9908787 CCC: $18.00
Published on Web 07/22/1999

```
        hhhhhhh hhh1hhhhhh hhhh  /\1/ \/\    /\2 /\/          /2a\        hhhhhhh hh2hhhhhhh
GC1   TPVSEKQLAE VVANTVTPLM KAQSVPGMAV AVIYQGKPHY YTFGKADIAA NKPVTPQTLF ELGSISKTFT GVLGGDAIAR   80
                      *
P99   TPVSEKQLAE VVANTITPLM KAQSVPGMAV AVIYQGKPHY YTFGKADIAA NKPVTPQTLF ELGSISKTFT GVLGGDAIAR   80

      h        h3ahh    h3b hh   hhh4h hh               hhhh h4ahhhhh               hhhhh5hhh
GC1   GEISLDDPVT RYWPQLTGKQ WQGIRMLDLA TYTAGGLPLQ VPDEVTDNAS LLRFYQNWQP QWKPGTTRLY ANASIGLFGA  160
          *
P99   GEISLDDAVT RYWPQLTGKQ WQGIRMLDLA TYTAGGLPLQ VPDEVTDNAS LLRFYQNWQP QWKPGTTRLY ANASIGLFGA  160

      hhh     hh hhh6hhhhh        /2b      h6ahh                    hh h7hh/2c\hh hhhh8hhhhh
GC1   LAVKPSGMPY EQAMTTRVLK PLKLDHTWIN VPKAEEAHYA WGYRDGKAVR AVRVSPGMLD AQAYGVKTNV QDMANWVMAN  240

P99   LAVKPSGMPY EQAMTTRVLK PLKLDHTWIN VPKAEEAHYA WGYRDGKAVR ---VSPGMLD AQAYGVKTNV QDMANWVMAN  237

      hh     hhh hhh9hhhhhh  /2d\  /2e \  /2f\     hhh10hhhh hh10ahh/2g                /\/3\
GC1   MAPENVADAS LKQGIALAQS RYWRIGSMYQ GLGWEMLNWP VEANTVVEGS DSKVALAPLP VAEVNPPAPP VKASWVHKTG  320

P99   MAPENVADAS LKQGIALAQS RYWRIGSMYQ GLGWEMLNWP VEANTVVEGS DSKVALAPLP VAEVNPPAPP VKASWVHKTG  317

      /\  /\/\4/ \/\  /\/\5 /\/\   hhh hhh11hhhhh h
GC1   STGGFGSYVA FIPEKQIGIV MLANTSYPNP ARVEAAYHIL EALQ  364

P99   STGGFGSYVA FIPEKQIGIV MLANTSYPNP ARVEAAYHIL EALQ  361
```

FIGURE 1: Amino acid sequences for the mature forms of GC1 (top line) and P99 β-lactamases. Differing residues at 16 and 88 are marked. The tripeptide insertion after 210 requires that numbering in text be based on the longer GC1 sequence. α and β secondary structures are indicated by hhh and /\/\/\, respectively, and include the numbering scheme used for class A and C β-lactamases (*10*).

structure of the GC1 enzyme and its comparison with the wild-type P99 enzyme.

MATERIALS AND METHODS

Expression and Purification of Enzyme. Escherichia coli AS226-51 cells carrying the pTTQ18K plasmid with the GC1 β-lactamase gene under the control of the *tac* promoter were grown in Terrific broth (*11*) containing 50 μg/mL kanamycin at 37 °C (*9*). In mid-logarithmic phase, isopropyl 1-thio-β-D-galactopyranoside was added to 0.5 mM final concentration, and the culture was continued for 12 h. The cells were harvested by centrifugation, and periplasmic content was liberated by lysozyme treatment. The periplasmic supernatant was dialyzed against three changes of 10 mM triethanolamine hydrochloride buffer at pH 7.0. Enzyme was purified in three chromatography steps with CM-Sephadex C-50 (Pharmacia), an Affi-Gel-10 (Bio-Rad) affinity column using (*m*-aminophenyl)boronic acid (*12*), and Sephadex G-25, as previously reported (*9*). The purity of pooled fractions was estimated to be more than 97% as judged by SDS−PAGE.

Crystallization. Crystals of the 39.4 kDa β-lactamase were grown at room temperature by the sitting-drop vapor diffusion method using 1:1 or 3:2 ratios of protein to reservoir solutions. Protein at 13.4 mg/mL was diluted with reservoir solution which contained 12.5−15% PEG[1] (M_r = 8000; Sigma Chemical Co., St. Louis, MO) and 0.05−0.1 M KH_2PO_4 at pH 5. Thin platelike crystals grew in 2 weeks to approximately 0.3 × 0.06 × 0.02 mm in size and had space group $P2_12_12$ with cell dimensions a = 78.0 Å, b = 69.5 Å, and c = 63.1 Å and one molecule in the asymmetric unit (2.17 Å^3/Da; 43% solvent volume). This unit cell is very similar to the orthorhombic cell reported for the wild-type β-lactamase from *E. cloacae* P99 at neutral pH (*13*). At higher pH values above pH 8 a prismatic form of GC1 grew in PEG with a monoclinic unit cell (a = 46.5 Å, b = 83.5 Å, c = 96.5 Å, β = 90.0°, and two molecules per asymmetric unit) that is apparently isomorphous with the cell found for the P99 enzyme at alkaline pHs (*10*).

Table 1: X-ray Data Collection and Reduction

temp (K)	100		
d_{min} (Å)	1.80	highest shell, d (Å)	1.86−1.80
observations	122470	observations	4591
unique reflections	31187	unique reflections	2568
completeness	0.96	completeness	0.80
av $I/\sigma(I)$	11.1	av $I/\sigma(I)$	5.1
$R_{merge}(I)$[a]	0.076	$R_{merge}(I)$[a]	0.142

[a] $R_{merge} = \sum|I_{av} - I_i|/\sum I_i$, where I_{av} is the average of all individual observations, I_i. The space group is $P2_12_12$.

X-ray Data Collection. A crystal of the orthorhombic form was flash frozen in a nitrogen gas stream to 100 K (Oxford Cryosystems) in a cryoprotectant containing 25% glycerol, 15.6% PEG 8000, and 50 mM potassium phosphate. Prior equilibration time in the cryoprotectant was 1 min. Data collection was performed at MacCHESS station A1 at the Cornell High Energy Synchrotron Source. A CCD area detector (Area Detector Systems Corp.) was used in 1K × 1K mode at a distance of 82 mm from the crystal. A total of 118° of data, made from 1° ϕ oscillations of 20−26 s each, was processed using the HKL programs (*14*) to give an overall completeness of 95.6% to 1.8 Å resolution and an R_{merge} (on intensities) equal to 7.6%. Data statistics are summarized in Table 1.

RESULTS

Structure Determination. The crystal structure was solved by molecular replacement using as a search model a molecule of the β-lactamase from *E. cloacae* P99 (*10*), Protein Data Bank entry 2BLT). The P99 enzyme has 359 residues in common with the 364 residues of the GC1 enzyme (Figure 1). The program AMoRe (*15*) was used with an integration radius of 27 Å for all data in the resolution range 8−4 Å. A single rotation solution was found 50% higher than the next solution. The translation search in the same resolution range

[1] Abbreviations: PEG, poly(ethylene glycol); rmsd, root of the mean of the squared deviations.

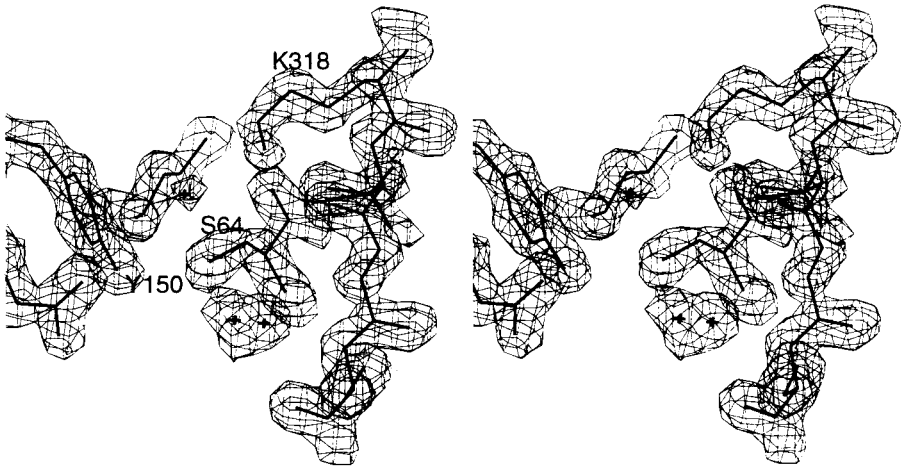

FIGURE 2: Stereoview of $2F_o - F_c$ electron density around the catalytic site as plotted by CHAIN (*18*). The contour level is 1.25σ. The dual conformation of Thr319 on β-strand B3 is seen. Waters are marked.

produced a correlation coefficient of 54.8%. Rigid-body refinement of this solution increased the correlation coefficient to 60.3% and gave an *R*-factor of 37.5%.

Structure Refinement. Simulated annealing refinement was initiated at 1500 K with X-PLOR version 3.8.5.1 (*16*). Data from 8.0 to 2.5 Å with F_o greater than $3\sigma(F)$ were used, with 5% of the data excluded for calculating R_{free} (*17*). Individual *B*-factors were initially set to 15 Å^2 for all atoms. After this stage the crystallographic and free *R*-factors were 27% and 32%, respectively. The initial electron density map using data from 21 to 1.8 Å was generally complete along the polypeptide chain, except for the region 212−216 where broken density was seen. (The insertion after 210 requires that numbering be based on the longer GC1 sequence.) Several cycles of manual fitting of the GC1 sequence (*6*) using the program CHAIN (*18*) were done to optimize backbone and side chain positions. To choose side chain rotamers and water positions, hydrogen-bonding patterns and *B*-factors were carefully monitored. Final annealing cycles were started at 500 K and included restraints on water positions.

Electron density maps failed to indicate unambiguous positions for five or six residues in the Ω loop, though significant, disconnected density was present in this region. Because of uncertainty, three residues (Arg213-Val214-Ser215) were excluded from the final model. Residues 216−220 have *B*-factors approaching 50 Å^2. For a model which includes 361 amino acid residues and 235 water molecules (*B*-factors <55 Å^2), the resulting crystallographic *R*-factor is 0.20 for all nonzero data in the range 8.0−1.80 Å. The R_{free} value is 0.23. Deviations of the protein model from ideality are 0.008 Å and 1.4° for covalent bonds and angles, respectively. Two conformations were observed for the side chains of residues Thr319 and Val329 on β-strands. Prolines 280 and 306 have the cis conformation, as in the P99 β-lactamase (*10*). Five of the six non-glycine residues having positive ϕ and ψ angles in the a_L region were seen also in the P99 enzyme. The sixth residue, Asp205, is five residues upstream from the insertion in the Ω loop. Refinement results are given in Table 2. The electron density map near the catalytic site is shown in Figure 2. The map unexpectedly showed a bridge of strong electron density connecting atom CE2 of Tyr150 and atom NZ of Lys67. Though the density was left unmodeled, we believe it to be a nitrogen atom resulting from the reaction of the protein with sodium azide bacteriostat present in the crystallizing buffer. Atomic coordinates have been deposited in the Protein Data Bank (entry 1GCE) at Rutgers University.

Table 2: Crystallographic Refinement

resolution range (Å)	8.0−1.8
no. of reflections used [$F > 0\sigma(F)$]	30206
R-factor	0.20
R_{free} factor[a]	0.23
rms deviations from ideality	
bond lengths (Å)	0.008
bond angles (deg)	1.4
planarity (deg)	1.3
mean *B*-factors (Å^2)	
protein	13.9
water	28.7
all atoms	15.1

[a] Calculated from 5% of the reflections omitted from the penultimate cycle of refinement. The standard *R*-factor for last cycle includes all reflections.

DISCUSSION

The extended-spectrum class C GC1 β-lactamase is a two-domain structure having a helical domain and a closely associated α-β domain. The β-lactam binding cavity lies between the two domains at the edge of a central β-strand that is part of a highly twisted nine-stranded antiparallel β-sheet (Figure 3).

GC1 and Its Comparison with the P99 β-Lactamase. The global structure of the GC1 β-lactamase is generally equivalent to that of the P99 enzyme (*10*), the wild-type β-lactamase which has been compared to smaller class A β-lactamases and to ancestral cell wall synthesizing enzymes inhibited by β-lactam antibiotics (*19*). Two conservative amino acid sequence differences at 16 (Ile to Val in GC1) and 88 (Ala to Pro) are seen also in other class C sequences. Val16 occurs on an internal surface of the N-terminal H1 helix, and Pro88 is found on an external segment following the H2 helix. Both of these amino acid changes are more than 20 Å distant from the reactive Ser64 and are not expected to influence binding or catalysis. A more significant change, the insertion of a three amino acid peptide, occurs after position 210 in the so-called Ω loop (189−226). This structure-altering insertion is unique among β-lactamases and will be discussed below.

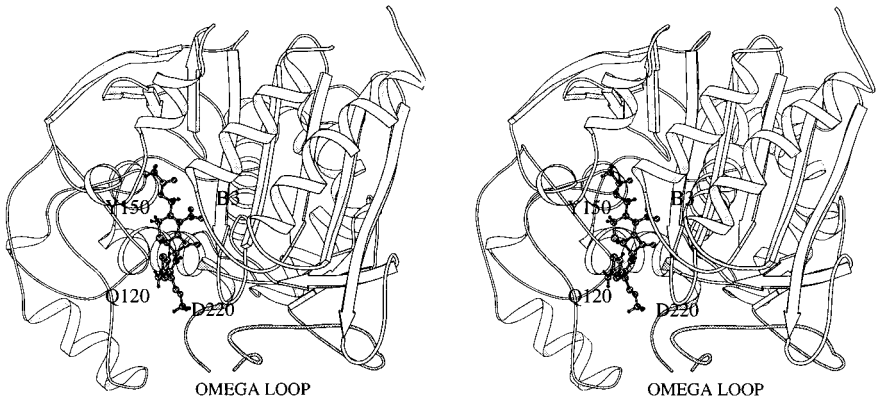

FIGURE 3: The GC1 β-lactamase drawn by MOLSCRIPT (*27*). Cefotaxime has been docked to show the position of the β-lactam binding site near Ser64 and strand B3. Unmodeled polypeptide 213−215 is omitted from the Ω loop at the bottom.

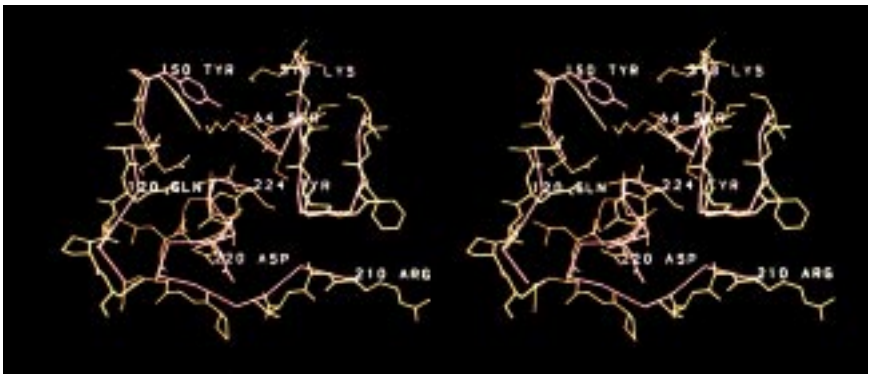

FIGURE 4: Stereoview of the overlay of the structure near the Ω loop in β-lactamases from GC1 and P99 (backbone dashed, red) drawn by FRODO (*28*). Side chain differences of Y150 and D220 are shown. The view is similar to that in Figures 2 and 3.

α-Carbon atoms of the GC1 and P99 enzymes overlay within an rmsd of 0.6 Å, excluding the three disordered residues in the Ω loop. For comparison, the overlay of GC1 with the less homologous (80%) class C β-lactamase of *E. coli* [Protein Data Bank entry 2BLS (*20*)] gives an rmsd of 0.8 Å. For the GC1/P99 pair the deviations greater than the rms value occur at the N-terminus and at 200−218 in the Ω loop region (Figure 4). In addition, there are differences in a loop containing Gln120 and in contact with the Ω loop. This produces a noticeable widening of the binding cavity. Distances from the B3 β-strand (318−324) across the cavity mouth to the two small loops containing Gln120 and Tyr150 are 0.6−1.4 Å larger in GC1.

The Ω *Loop*. The large Ω loop at the bottom of the binding cavity (Figures 3 and 4) is a structural feature that helps to differentiate the class C enzymes from the smaller class A enzymes (*19*). In each class the loop forms a wall of the binding cavity, but it runs in opposite directions across the cavity. In the class A cavity, the helical portion of the Ω loop hinders the binding of β-lactams with large rigid oxyimino substituents on the β-lactam ring. In the class C cavity, the short helical part of the loop is positioned differently and is somewhat less an obstruction to bulky side chains.

The Ω loop in class A β-lactamases contains the catalytic base, Glu166, required for deacylation. Any mutational changes in the Ω loop, arising to accommodate larger R groups on the substrate, for example, may reduce activity if a large movement of the Glu166 results from the mutation. The crystal structure of the D179N mutant of the class A *Staphylococcus aureus* enzyme showed a disordered Ω loop that could explain the enzyme's reduced deacylation rate (*21*), and a loopless mutant of the same β-lactamase showed increased binding of bulky cephalosporins, also with poor deacylation (*22*). However, in class C β-lactamases the loop contains no residue functioning as a catalytic base (*23, 24*). Therefore, any mutational changes in the Ω loop can influence catalysis only indirectly.

The electron density map of GC1 shows a localized disorder in the Ω loop at residues 213−215, the part of the loop nearest the expected position of C7(3) substituents of oxyimino cephalosporins and monobactams. These disordered residues include one amino acid of the tripeptide insertion 211−213. This disorder is consistent with earlier measurements of thermal stability showing that the GC1 mutant is less stable than the P99 wild type (*9*). Further work with engineered mutants of GC1 indicated that the exact amino acid sequence of the insertion appeared to be less important than the *length* of the insertion. A trialanine insertion resulted in the same lowering of thermal stability. These results were taken to suggest that structural instability exists in the Ω loop of the mutant. This instability produces an increase in oxyimino β-lactam hydrolysis by increasing the rate of deacylation. Accordingly, the hydrolysis of traditional β-lactams, or small inhibitors, was not changed because their smaller substituents would not contact the Ω loop, even if it is more floppy.

These findings of the Sawai group can now be combined with our crystallographic results. We see that the path of the Ω chain up to and including Ala208-Val209-Arg210 in the wild-type enzyme is followed by the mutant polypeptide. In both enzymes the Arg210 side chain is well sandwiched

Table 3: Catalytic Site Distances (Å)[a]

A	Ser64OG	Lys67NZ	2.94 (3.11)
B	Tyr150OH	Lys67NZ	2.79 (2.94)
C	Ser64OG	Tyr150OH	3.45 (3.20)
D	Tyr150OH	Lys318NZ	6.42 (3.05)
E	Lys67NZ	Asn152OD1	2.94 (2.62)
F	Ser64N	Ser321N	4.00 (3.75)
G	Ser64OG	Lys318NZ	4.54 (4.75)
L1	Ser64N	W404	2.78 (3.60)
L2	Ser321N	W404	2.86 (2.85)
	Tyr150OH	W551	3.44
	Lys318NZ	W551	3.09

[a] The lettering convention is from ref *19*. The average distance for two molecules in the asymmetric unit of the P99 β-lactamase is in parentheses (*10*).

between parallel aromatic side chains of Tyr202 and Trp204, and its guanidinium group is anchored by hydrogen bonds to backbone carbonyl groups. Arg210 is further held by a hydrogen bond from its amide group to Glu61. Thus, this wild-type tripeptide is secured by the surrounding structure and not easily altered, consistent with the mutagenesis and modeling studies by Nukaga et al. (*6*). The tandem mutation occurs immediately *after* Ala208-Val209-Arg210, in a solvent-exposed region of the loop with no links to the rest of the enzyme. Consequently, part of the inserted tripeptide and the two or three residues after it have high *B*-factors or are disordered.

Further, this perturbation is transmitted to the following segment of the loop from 217 to 222, where conformational changes are seen relative to the wild-type P99 enzyme. A backbone peptide flip occurs in a β turn between Met218 and Leu219. The carboxylic acid side chain of Asp220, solvated in P99, now rotates about 180° toward the binding cavity and hydrogen bonds to the hydroxyl group of Tyr224.

Neighboring protein structure is affected by the expansion of the Ω loop. The smaller Gln120 loop, in contact with the Ω loop near Met218, shifts more than 1 Å to widen the mouth to the binding cavity. The bottom of the B3 β-strand, forming an edge of the binding cavity, moves 0.5−0.6 Å. It is not entirely clear how these movements and amplified motions could facilitate hydrolysis. Generally, the changes may open the cavity for entry of larger substrates, may allow better positioning of the acyl intermediate for attack by a water molecule, or may permit more rapid departure of the hydrolysis product.

Catalytic Site. The disorder in the Ω loop and the alterations in the surrounding structure do not disturb the core residues known to be involved with substrate binding and catalysis. An overlay of the six catalytic site residues Ser64, Lys67, Tyr150, Asn152, Lys318, and Ser321 shows close fit (0.37 Å rmsd) with those in the P99 enzyme. Distances between these groups differ little from P99 (Table 3), with the important exception of Tyr150, whose side chain has rotated 25−30° relative to P99 (Figure 4). This rotation is probably due to pH differences in the GC1 and P99 crystals, which are at approximately pH 5 and 8, respectively. While in P99 an anionic hydroxyl group of Tyr150 (*25*) electrostatically bonds with the ammonium group of Lys318, in GC1 the hydroxyl group may be protonated and no longer interacts with Lys318. Therefore, the movement of Tyr150 can be correlated with the crystal pH values at 6 or 8, and it is consistent with the suggestion that a catalytic role for this residue is dependent on its having a lower than normal pK_a value (*26*). Confounding the analysis of distances in the catalytic site is the unusual one-atom covalent bridge between Tyr150 and Lys67 (see Results). The position of Tyr150 at the low pH, relative to P99, may have placed the side chain in a favorable orientation for the presumed reaction with azide ion.

In this substrate-free binding site a water molecule binds between the backbone amides of Ser64 and Ser321 in an oxyanion hole, the width of which is significantly narrower than in class A β-lactamases (*19*). The water density has ellipsoidal shape and was modeled in two positions 1.3 Å apart (W404 and W423). Possibly related is the fact that two conformations are seen for the side chain of Thr319, which lies near the oxyanion hole. Because of the threonine's likely interaction with anionic groups of β-lactams and inhibitors (*25*, *26*), the hydroxyl group of Thr319 is expected to have a single conformation in complexes. As the disordered Ω loop is rather distant from these catalytic site residues, it is not unexpected that small inhibitors such as sulbactam and *m*-aminophenylboronic acid, each lacking large substituents, are found to bind to this GC1 mutant with the same K_i as for the wild-type P99 β-lactamase (*9*).

ACKNOWLEDGMENT

We thank the staff at the MacCHESS facility at the Cornell High Energy Synchrotron Source for help in collecting X-ray data (under Grant NSF-DMR97-13424) and P. C. Moews and M. A. McDonough for assistance with data processing.

REFERENCES

1. Bulychev, A., Massova, I., Miyashita, K., and Mobashery, S. (1997) *J. Am. Chem. Soc. 119*, 7619−7625.
2. Page, M. I., and Laws, A. P. (1998) *Chem. Commun.*, 1609−1617.
3. Bush, K., Jacoby, G. A., and Medeiros, A. A. (1995) *Antimicrob. Agents Chemother. 39*, 1211−1233.
4. Frere, J.-M. (1995) *Mol. Microbiol. 16*, 385−395.
5. Massova, I., and Mobashery, S. (1998) *Antimicrob. Agents Chemother. 42*, 1−17.
6. Nugaka, M., Haruta, S., Tanimoto, K., Kogure, K., Taniguchi, K., Tamaki, M., and Sawai, T. (1995) *J. Biol. Chem. 270*, 5729−5735.
7. Matagne, A., Lamotte-Brasseur, J., and Frere, J.-M. (1998) *Biochem. J. 330*, 581−598.
8. Petrosino, J., Cantu, C., and Palzkill, T. (1998) *Trends Microbiol. 6*, 323−327.
9. Nukaga, M., Taniguchi, K., Washio, Y., and Sawai, T. (1998) *Biochemistry 37*, 10461−10468.
10. Lobkovsky, E., Moews, P. C., Liu, H., Zhao, H., Frere, J.-M., and Knox, J. R. (1993) *Proc. Natl. Acad. Sci. U.S.A. 90*, 11257−11261.
11. Tartof, K. D. (1992) *Methods Enzymol. 216*, 574−584.
12. Cartwright, S. J., and Waley, S. G. (1984) *Biochem. J. 221*, 505−512.
13. Charlier, P., Dideberg, O., Frere, J.-M., Moews, P. C., and Knox, J. R. (1983) *J. Mol. Biol. 171*, 237−238.
14. Otwinowski, Z., and Minor, W. (1997) *Methods Enzymol. 276*, 307−326.
15. Navaza, J. (1994) *Acta Crystallogr. A50*, 157−163.
16. Brunger, A. T. (1992) *X-PLOR: A system for X-ray crystallography and NMR, Version 3.1*, Yale University Press, New Haven, CT.
17. Brunger, A. T. (1992) *Nature 355*, 472−475.
18. Sack, J. S. (1988) *J. Mol. Graphics 6*, 224−225.

19. Knox, J. R., Moews, P. C., and Frere, J.-M. (1996) *Chem. Biol. 3*, 937−947.
20. Usher, K. C., Blaszczak, L. C., Weston, G. S., Shoichet, B. K., and Remington, S. J. (1998) *Biochemistry 37*, 16082−16092.
21. Herzberg, O., Kapadia, G., Blanco, B., Smith, T. S., and Coulson, A. (1991) *Biochemistry 30*, 9503−9508.
22. Banerjee, S., Pieper, U., Kapadia, G., Pannell, L. K., and Herzberg, O. (1998) *Biochemistry 37*, 3286−3296.
23. Tsukamoto, K., Kikura, R., Ohno, R., and Sawai, T. (1990) *FEBS Lett. 264*, 211−214.
24. Tsukamoto, K., Ohno, R., Nukaga, M., and Sawai, T. (1992) *Eur. J. Biochem. 207*, 1123−1127.
25. Lobkovsky, E., Billings, E. M., Moews, P. C., Rahil, J., Pratt, R. F., and Knox, J. R. (1994) *Biochemistry 33*, 6762−6772.
26. Oefner, C., D'Arcy, A., Daly, J. J., Gubernator, K., Charnas, R. L., Heinze, I., Hubschwerfen, C., and Winkler, F. K. (1990) *Nature 343*, 284−288.
27. Kraulis, P. (1991) *J. Appl. Crystallogr. 24*, 946−950.
28. Jones, T. A. (1985) *Methods Enzymol. 115*, 157−170.

BI9908787